

## CO Adsorption on Au(110)–(1 × 2): An IRAS Investigation

Douglas C. Meier,<sup>†</sup> V. Bukhtiyarov,<sup>†,‡</sup> and D. Wayne Goodman<sup>\*,†</sup>

Department of Chemistry, Texas A&M University, P.O. Box 30012, College Station, Texas 77842-3012, and  
Boreskov Institute of Catalysis, Lavrentieva prospekt, 5, Novosibirsk, 630090, Russia

Received: April 24, 2003

IRAS studies of CO adsorption on the Au(110)–(1 × 2) surface were performed as a function of CO pressure and sample temperature. It was found that with increasing coverage, the CO IRAS absorption shifts red from 2118 to 2108 cm<sup>-1</sup>. Clausius–Clapeyron data analysis yielded a heat of CO adsorption ( $-\Delta H_{\text{ads}}$ ) of 10.9 kcal/mol at low coverages and 7.8 kcal/mol at coverages greater than 19%.

### Introduction

Improvement of existing catalysts and finding new catalysts for desired products is an ever-present challenge. Recently, one such breakthrough was made using one of the most unlikely of metals, gold. Long sought for its noble metal properties, much attention has recently been paid to the potential uses for gold deposited on metal oxides in catalysis.<sup>1–3</sup> While a number of these recent discoveries have provided electronic, reactivity, and particle size information on these systems, questions remain concerning the role of the metal in the catalytic process, the crystal structure of the particles, and the effects on the activity, if any, of the various support materials used. These questions linger in part due to the complexity of these systems, where substrate material and morphology as well as gold particle size and morphology are variable and difficult to control and identify on high surface area catalysts. We propose an approach in which the complex system is dissected into simple, well-defined components, which are then studied separately using ultrahigh vacuum (UHV) surface science techniques. The information derived from these studies, when compared to analogous information collected from the complex systems and more complex models, will result in a broadened understanding of the catalytic properties of supported gold and allow for those desirable effects to be optimized. This study addresses CO adsorption on the gold single crystal as a first step in this approach.

The primary technique chosen for this work is infrared reflection absorption spectroscopy (IRAS) of CO adsorbed to the gold single crystal. This method affords exceptional advantages en route to understanding the chemical and physical properties of gold systems. The chemical properties of the substrate can be inferred by studying the absorbance frequency of the CO probe molecule and its shift as a function of coverage.<sup>4,5</sup> The heats of adsorption ( $-\Delta H_{\text{ads}}$ ) of CO can also be measured as a function of coverage using a Clausius–Clapeyron treatment of the absorbance intensities.<sup>6</sup> Most importantly, since IRAS is a photon technique that is not restricted to use in the UHV environment, it provides a ready bridge between data collected from both idealized and complex

catalytic systems studied at a range of pressures from UHV to ambient.

Some relevant studies have already been performed using UHV vibrational techniques to observe CO interacting with a variety of gold systems. Kottke et al.<sup>7</sup> used IRAS to study CO adsorption to evaporated gold films. By using a multiple-reflection scheme and a high (>0.01 Torr) CO pressure to enhance signal-to-noise, a CO band was observed at 2120 cm<sup>-1</sup>, shifting to 2115 cm<sup>-1</sup> at higher CO pressure. Since the peak appears to shift continuously as a function of pressure, it was proposed that interactions between adsorbed CO at equivalent adsorption sites cause the metal–carbon bond to weaken and thus produce the shift. This study also included adsorption enthalpies for varying coverages by employing a Clausius–Clapeyron analysis of isothermal data. The average result of 13.4 kcal/mol was constant from 10% to 60% coverage.

Later investigations that used IRAS to observe the interaction of CO with a vicinal cut crystal showed that the band shifts and adsorption energies of this more highly defined system were strikingly different. Ruggiero et al.<sup>8</sup> used surface potential measurements to gauge the amount of CO adsorbed to a Au-(332) crystal. By performing a Clausius–Clapeyron analysis on isobaric desorption data and confirming the result with temperature-programmed desorption (TPD) data analyzed using the Redhead approximation,<sup>9</sup> two separate coverage-dependent adsorption states were discovered. While the low coverage result also yielded an adsorption enthalpy of 13 kcal/mol, the heat of adsorption abruptly dropped to below 5 kcal/mol at higher coverages. A similar analysis of isobaric desorption of CO from Au(100) performed by McElhiney et al.<sup>10</sup> yielded a similar two-phase adsorption profile. IRAS data collected from this single crystal showed a single peak at 2124 cm<sup>-1</sup> that shifted with higher coverage to 2110 cm<sup>-1</sup>.<sup>8</sup> This slight deviation from the thin-film data shows that differing gold morphologies can result in differing CO IRAS signals, which could then aid in the identification of morphology.

Au(110)–(1 × 2) serves as a simple model for the more complex dispersed gold catalyst. The benefits of using this reconstructed system are its ease of formation from Au(110) single crystals and its open structure, which amounts to a regular array of (111) facets with a step-edge made up of 6-coordinate atoms every fourth atomic row.<sup>11–14</sup> This high population of low coordination sites provides ample opportunity for comparison with the behavior of adsorbed gold particles, which are also

\* Author to whom correspondence should be addressed. E-mail: goodman@mail.chem.tamu.edu.

<sup>†</sup> Texas A&M University.

<sup>‡</sup> Boreskov Institute of Catalysis.

expected to have a large percentage of low coordination sites, on the basis of scanning tunneling microscopy (STM) data.<sup>15</sup> Such systems have been reported to cause frequency shifts in the vibrational energy of adsorbed CO.<sup>16</sup> This system provides an excellent benchmark for comparing support effects for oxide-supported gold particles.

Chemisorption of CO on Au(110)–(1 × 2) was studied at 300 K at high CO pressure ( $1 \times 10^{-1}$  Torr to  $1 \times 10^2$  Torr) using polarization modulation (PM)-IRAS.<sup>17</sup> These experiments reveal a single pressure-insensitive absorption feature at 2110  $\text{cm}^{-1}$  that decreases in intensity over a period of several hours before disappearing entirely, an effect accompanied by the appearance of surface carbon. Furthermore, CO pressures exceeding  $1 \times 10^{-5}$  Torr are observed via scanning tunneling microscopy (STM) to cause reconstruction to a roughened structure of disrupted Au(110)–(1 × 2) ridges. Furthermore, CO oxidation experiments have previously been performed on the unreconstructed Au(110) surface, on which it was inferred by TPD that  $-\Delta H_{\text{ads}}$  for CO on the surface was less than 8 kcal/mol.<sup>18</sup> Comparison of this inference with thermodynamic data collected from CO adsorption on the reconstructed surface provides a useful comparison to gauge morphological effects on binding in gold systems.

## Experimental Section

This study was performed in a UHV chamber equipped with a Perkin-Elmer Auger electron (AES) spectrometer, a UTI Instruments quadrupole mass analyzer, a Physical Electronics low-energy electron diffraction (LEED) spectrometer, a Perkin-Elmer ion sputtering gun, and an infrared cell separated from the main chamber by a sliding seal. This apparatus has been described in greater detail elsewhere.<sup>19,20</sup> The infrared cell is fitted with flange-mounted  $\text{CaF}_2$  windows in the infrared beam path. While the sample is in the infrared cell, it may be pressurized independently of the main UHV chamber, allowing experiments to be performed at elevated pressures without affecting the main chamber vacuum. Pressure in both the main chamber and in the infrared cell was measured using a Granville-Phillips ionization gauge.

Oxygen (99.99%, BotCo, Bryan, TX) and carbon monoxide (99.99%, Matheson Gas Products) were further purified by fractional condensation and transferred to glass bulbs attached to the chamber gas manifold. The CO bulb was immersed in liquid nitrogen throughout the experiments in order to reduce the occurrence of volatile metal carbonyl contamination. The Au(110) single crystal (Accumet Materials Co.) was mounted by spot-welding a tantalum wire loop around the edge of the crystal and a type C thermocouple (H. Cross Co.) to the back of the sample. This mount was attached to a cylindrical probe with both power and thermocouple feedthroughs, allowing for both controlled resistive heating of the sample to 1500 K and liquid nitrogen cooling to 90 K. The sample was cleaned prior to use by cycles of annealing at 600 K in  $5 \times 10^{-7}$  Torr oxygen followed by argon ion sputtering until Auger electron spectroscopy (AES) confirmed a gold surface free of carbon and oxygen. The Au(110)–(1 × 2) reconstruction was formed by cycles of argon ion sputtering at room temperature followed by vacuum annealing to 1000 K until a sharp (1 × 2) LEED pattern was obtained.

IRAS spectra were collected using the Mattson Cygnus 100 spectrometer in single beam mode with external optics aligned for an incident angle 85 degrees from sample normal. Detection was via a MCT detector. All spectra were averages of 512 scans at 4  $\text{cm}^{-1}$  resolution. The absorbance spectra of CO/Au(110)–

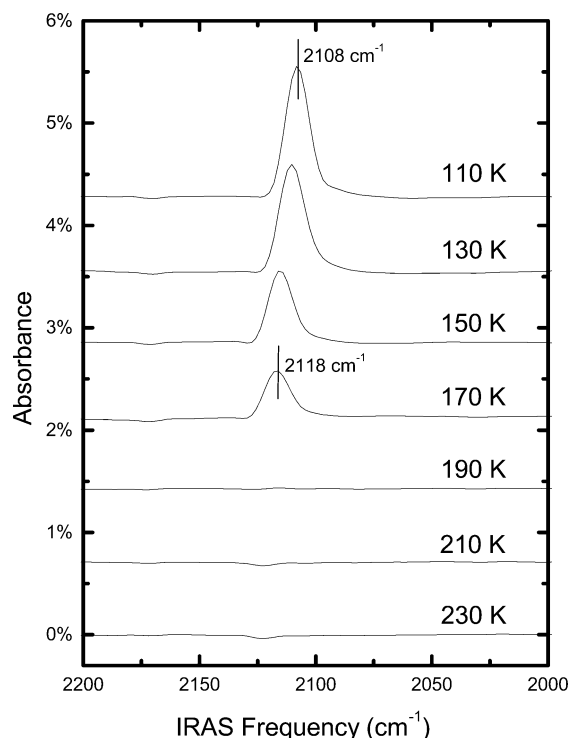


Figure 1.  $1.3 \times 10^{-8}$  Torr CO/Au(110)–(1 × 2).

(1 × 2) were taken as the inverse log of the ratios of the single beam emissivities at the recorded temperatures and CO pressures over the emissivities recorded at 300 K and at  $1 \times 10^{-9}$  Torr background pressure. A series of isobaric spectra from  $1 \times 10^{-8}$  Torr to  $1 \times 10^{-4}$  Torr were collected at temperatures starting at 100 K and increasing by 10 K increments until no CO signal was observed.

## Results and Discussion

Figure 1 shows a series of IRAS data acquired at  $1.3 \times 10^{-8}$  Torr CO on the reconstructed gold surface at a range of temperatures. At the low coverage limit, the CO absorbance is a single feature at 2118  $\text{cm}^{-1}$ . As the temperature is decreased, leading to an increase in coverage, the feature red-shifts to 2108  $\text{cm}^{-1}$  at saturation, in close agreement with Jugnet.<sup>17</sup> Figure 2 shows a similar series collected at a CO pressure of  $10^{-4}$  Torr. The red-shift with increasing coverage is the same as that seen at low pressure, but the energies of the features as a function of coverage exhibit a slight red-shift (2  $\text{cm}^{-1}$ ) at the higher pressure.

The completed isobaric series are reorganized into isotherms in Figure 3. The integrated peak intensities are estimated to grow roughly linearly with respect to CO coverage up to  $\theta = 0.5$ . This estimation has been used in previous studies of CO adsorption to Cu(110), which is a Group IB analogue of Au(110).<sup>4,21</sup> Other studies of CO adsorption on late transition metals reveal similar relationships between coverage and infrared absorption intensity.<sup>22,23</sup> This effect has been attributed to depolarization due to interadsorbate interactions, which arise from a combination of surface ordering, dipole–dipole interactions, and through changing interactions with the substrate as coverage increases. Due to the complexities inherent in such interactions, simple models such as the Langmuir isotherm fit poorly to the data; smooth curves are included as guides to the eye as well as aids to interpolation of isosteres.

A series of isosteres are plotted in Figure 4 for every 1.7% of CO coverage up to and including 34% (where the coverage

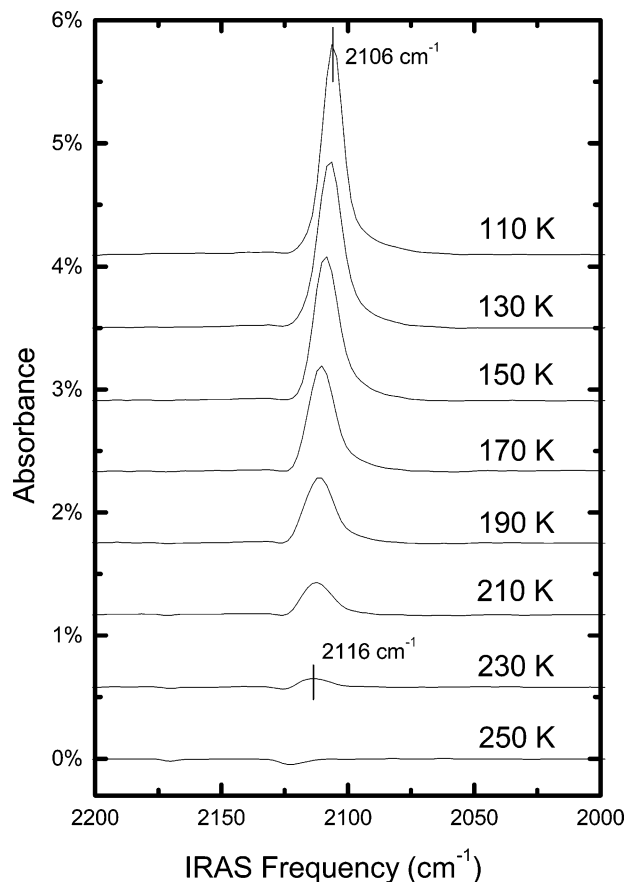


Figure 2.  $1 \times 10^{-4}$  Torr CO/Au(110)-(1  $\times$  2).

approximation is still safely valid). From the slopes of these plots, the heat of adsorption of CO as a function of surface coverage was calculated via a Clausius–Clapeyron analysis. The  $-\Delta H_{\text{ads}}$  for CO adsorption is 10.9 kcal/mol at the zero coverage limit and 7.8 kcal/mol at the high CO coverages (Figure 5). By fitting a Boltzmann distribution to these data, the transition from higher energy adsorption to lower energy adsorption was found to occur at  $\theta = 0.19$ .

The results for absorption frequency as a function of coverage agree well with prior studies, exhibiting only a slight overall red-shift from the CO/Au(332) spectra<sup>8</sup> and exactly that measured for CO/Au(110)-(1  $\times$  2) under high CO pressure and temperature.<sup>17</sup> The coverage dependence of the absorbance frequency can be explained as the result of offsetting effects, as was shown on Cu(110).<sup>4</sup> For this Au(110) Group IB analogue, a small (6  $\text{cm}^{-1}$ ) blue-shift with increasing coverage was observed to be due to a large (about 50  $\text{cm}^{-1}$ ) blue dipole shift and a nearly equal red chemical shift, which has been assigned to  $2\pi_b$  broadening across the Fermi level<sup>4</sup> in keeping with the Blyholder model<sup>24</sup> of CO absorption, which consists of the slightly antibonding CO 5 $\sigma$  transferring electron density to the metal valence while the metal d orbitals perform electron back-donation to the strongly antibonding CO  $2\pi_b$ . To summarize this hypothesis, a  $2\pi_b$  below the Fermi level causes a blue-shift when broadened, an explanation consistent with reduced  $\pi$ -back-bonding. On the other hand, a  $2\pi_b$  above the Fermi level results in a red-shift when broadened, which is a result consistent with the data of this study. Qualitatively, the shifts should be similar for metals in the same group.

If one is to believe, however, that the CO  $2\pi_b$  lies above the Fermi edge, then it must follow that the preponderance of the binding occurs in 5 $\sigma$  transfer to the gold valence, a band that is already filled. Furthermore, such  $\sigma$  donation-dominated bonding should cause a slight blue-shift in the CO vibrational frequency; in fact, these spectra are slightly red-shifted from the gas-phase value of 2143  $\text{cm}^{-1}$ . Models designed to explain these discrepancies invoke a “wall effect”<sup>25–27</sup> wherein steric repulsion between the CO 5 $\sigma$  and the filled metal d orbitals acts as a barrier to vibration. This barrier narrows the anharmonic oscillator potential well, causing a blue-shift in the vibrational frequency. Other interactions between the surface and the molecule, such as the electron transfer in bonding and changes in polarization, then work to lower the vibrational energy. Ongoing ab initio computations of CO adsorbed on a Au(100) cluster suggest a strong wall effect, a weak 5 $\sigma$  bond, and a significant  $2\pi_b$  back-bond.<sup>28</sup> This treatment also better explains the enhanced reactivity observed for CO on gold, since electron

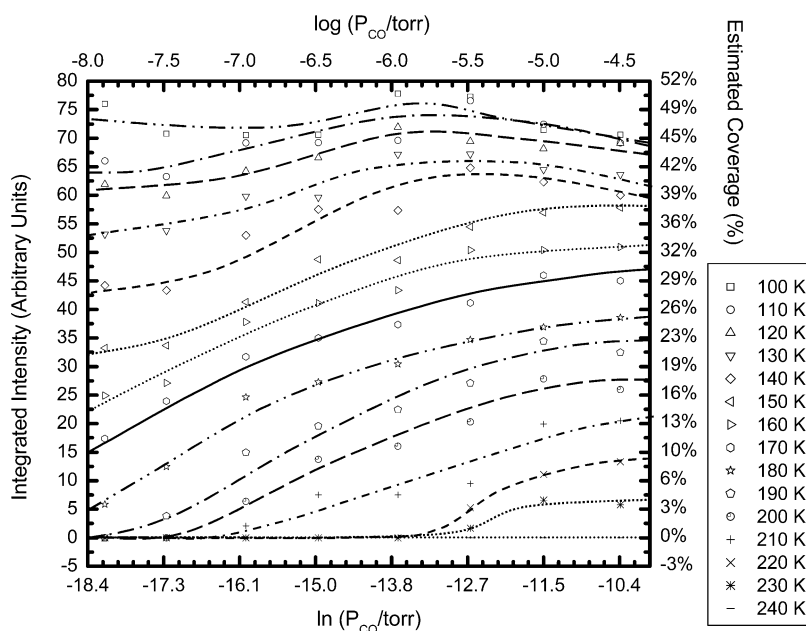
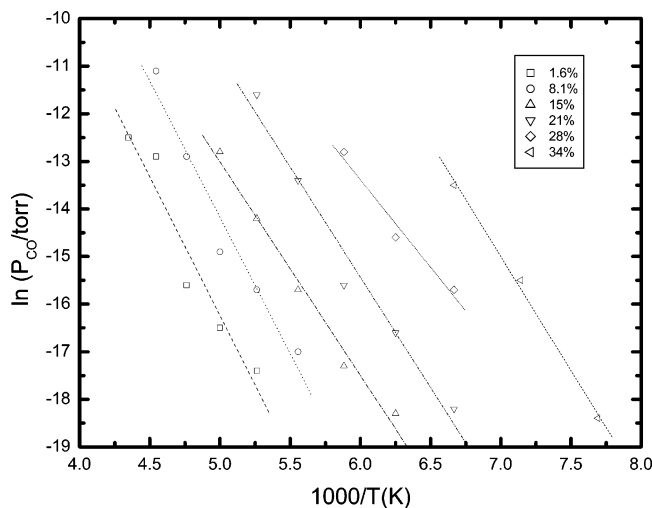
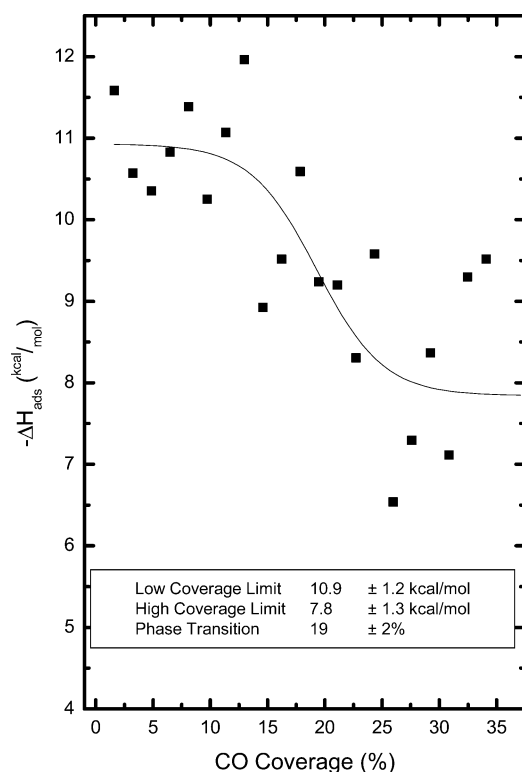


Figure 3. CO adsorption isotherms on Au(110)-(1  $\times$  2). Maximum absorbance is estimated at 50% coverage. Traces are guides to the eye and to assist in the interpolation of isosteres.



**Figure 4.** Representative isosteric plots for the CO/Au(110)-(1 × 2) system.



**Figure 5.** Heats of adsorption ( $-\Delta H_{\text{ads}}$ ) as a function of coverage for CO/Au(110)-(1 × 2). Trace is a guide to the eye only.

transfer into the antibonding  $2\pi_b$  orbital stretches the bond, lowering the activation energy for oxidation.

Finally, the thermodynamic results exhibit two distinct coverage-dependent adsorption energies, which is in agreement with other single-crystal results for gold surfaces. It is notable that the transition at 19% coverage (about 3 kcal/mol) is smaller than that observed for other gold surfaces in the literature (from 6 to 8 kcal/mol).<sup>8,10</sup> Also notable is the much higher adsorption energy (10.9 kcal/mol) than that inferred by Outka et al. (<8

kcal/mol),<sup>18</sup> showing that gold morphology plays a significant role in CO bonding energy, if not vibrational frequency. In this case, the effect is likely due to the lower coordination number of the surface gold atoms on the reconstructed surface compared to the unreconstructed surface.

## Conclusion

This study has provided information on the adsorption energies and vibrational dynamics of CO/Au(110) systems. The CO vibrational frequencies ( $2108\text{ cm}^{-1}$  to  $2118\text{ cm}^{-1}$ ) are in good agreement with prior work, which as a whole indicates environmental insensitivity of the CO vibrational frequency. However, the increased heat of adsorption observed in this work compared to prior single-crystal studies (10.9 kcal/mol compared to <8 kcal/mol) implies that lower gold coordination numbers are critical to stronger bonds to CO. Consideration of two bonding schemes suggests that back-bonding to the CO  $2\pi_b$  dominates the interaction and may dominate the subsequent chemistry that occurs in gold systems.

**Acknowledgment.** We acknowledge with pleasure the support of this work by the Department of Energy, Office of Basic Energy Sciences, Division of Chemical Sciences, Robert A. Welch Foundation, and the Texas Advanced Technology Program under Grant No. 010366-0022-2001.

## References and Notes

- (1) Haruta, M. *Catal. Today* **1997**, 36, 153.
- (2) Haruta, M.; Tsubota, S.; Kobayashi, T.; Kageyama, H.; Genet, M. J.; Delmon, B. J. *Catal.* **1993**, 144, 175.
- (3) Bond, G. C.; Thompson, D. T. *Gold Bull.* **2000**, 33, 41.
- (4) Woodruff, D. P.; Hayden, B. E.; Prince, K.; Bradshaw, A. M. *Surf. Sci.* **1982**, 123, 397.
- (5) Hollins, P.; Pritchard, J. *Surf. Sci.* **1979**, 89, 486.
- (6) Truong, C. M.; Rodriguez, J. A.; Goodman, D. W. *Surf. Sci. Lett.* **1992**, 271, L385.
- (7) Kottke, M. L.; Greenler, R. G.; Tompkins, H. G. *Surf. Sci.* **1972**, 32, 231.
- (8) Ruggiero, C.; Hollins, P. J. *Chem. Soc., Faraday Trans. 2* **1996**, 92, 4829.
- (9) Redhead, P. A. *Vacuum* **1962**, 12, 203.
- (10) McElhiney, G.; Pritchard, J. *Surf. Sci.* **1976**, 60, 397.
- (11) Binnig, G.; Rohrer, H.; Gerber, C.; Weibel, E. *Surf. Sci. Lett.* **1983**, 131, L379.
- (12) Hoefner, C.; Rabalais, J. W. *Surf. Sci.* **1998**, 400, 189.
- (13) Moritz, W.; Wolf, D. *Surf. Sci. Lett.* **1979**, 88, L29.
- (14) Garafalo, M.; Tosatti, E.; Ercolessi, F. *Surf. Sci.* **1987**, 188, 321.
- (15) Valden, M.; Lai, X.; Goodman, D. W. *Science* **1998**, 281, 1647.
- (16) Grunwaldt, J. D.; Maciejewski, M.; Becker, O. S.; Fabrizioli, P.; Baiker, A. *J. Catal.* **1999**, 186, 458.
- (17) Jugnet, Y.; Cadete Santos Aires, F. J.; Deranlot, C.; Piccolo, L.; Bertolini, J. C. *Surf. Sci. Lett.* **2002**, 521, L639.
- (18) Outka, D. A.; Madix, R. J. *Surf. Sci.* **1987**, 179, 351.
- (19) Leung, L. W. H.; He, J. W.; Goodman, D. W. *J. Chem. Phys.* **1990**, 93, 8328.
- (20) Campbell, R. A.; Goodman, D. W. *Rev. Sci. Instrum.* **1992**, 63, 172.
- (21) Horn, K.; Pritchard, J. *Surf. Sci.* **1977**, 63, 244.
- (22) Ryberg, R. *Surf. Sci.* **1982**, 114, 627.
- (23) Hoffmann, F. M. *Surf. Sci. Rep.* **1983**, 3, 107.
- (24) Blyholder, G. *J. Phys. Chem.* **1964**, 68, 2772.
- (25) Bagus, P. S.; Muller, W. *Chem. Phys. Lett.* **1985**, 115, 540.
- (26) Bagus, P. S.; Pacchioni, G. *Electrochim. Acta* **1991**, 36, 1669.
- (27) Freund, H.-J.; Neumann, M. *Appl. Phys. A* **1988**, 47, 3.
- (28) Bagus, P. S. Personal communication.